AUTONOMOUS ORBIT DETERMINATION AND NAVIGATION FOR FORMATIONS OF CUBESATS BEYOND LEO

Massimiliano Vasile[*], Francesco Torre[†], Romain Serra[‡], and Stuart Grey[§]

This paper investigates the use of the Time Of Arrival (TOA) and Doppler shift to allow a small formation of CubeSats to navigate beyond low Earth orbit (LEO). The idea is to use a one way communication, from one or more ground station to two or more CubeSats, to reconstruct an estimation of the position and velocity of the formation with respect to Earth. The paper considers the use of the difference in TOA and Doppler measurements to mitigate the error introduced by the onboard clock. These measurements are combined with inter-satellite distance and velocity measurements based on a two-way communication between pairs of spacecraft. The paper will provide an estimation of the error in position and velocity that can be obtained by a combination of these measurements. The reference case for these analyses will be a mission to the Moon.

INTRODUCTION

There is a growing interest in using nanosatellites (like CubeSats) beyond LEO. From the proposed NASA Mars mission MarCO[1] to more recent missions studies for CubeSats to the Moon and asteroids, the goal is to achieve significant scientific results with small, low-cost and compact spacecraft. The authors, in 2012, proposed a mission to the Moon with a low cost CubeSat that was employing a hybrid propulsion system. The challenge in all these cases is to achieve mission objectives with limited resources.

Given the low cost of the platform some limitations can be mitigated by using more than one nanosatellite working in team and distributing tasks and resources. The paper is proposing a combination of measurements that can be used to autonomously determine position and velocity of CubeSats flying in formation in deep space or in the vicinity of a minor body. The limited power on-board a CubeSat might not be sufficient to implement traditional tracking techniques for orbit determination based on ground support (Differential One-way Range (DOR) or delta-DOR for example). Furthermore, the precision of the clocks on-board a CubeSat do not generally allow for one way ranging and range rate measurements with sufficient accuracy if no synchronization strategy is applied.

The paper is investigating the possibility to exploit the inter-satellite link between two, or more CubeSats, together with different combinations of Time Of Arrival (TOA), Time Difference Of

[*]Professor, Mechanical & Aerospace Engineering, University of Strathclyde, G11XJ 75 Montrose Street Glasgow UK.
[†]PhD candidate, Mechanical & Aerospace Engineering, University of Strathclyde, G11XJ 75 Montrose Street Glasgow UK.
[‡]Research Fellow, Mechanical & Aerospace Engineering, University of Strathclyde, G11XJ 75 Montrose Street Glasgow UK.
[§]Lecturer, Mechanical & Aerospace Engineering, University of Strathclyde, G11XJ 75 Montrose Street Glasgow UK.

Arrival (TDOA), Frequency Of Arrival (FDOA) and optical navigation to determine their position and velocity with respect to a known beacon. The approach is similar to known techniques for the localization of a source given the known position of different receivers[2–5] albeit it assumes one or more known emitters and unknown receivers. The signal emitted from one or more ground stations (the known beacons), and received by two or more spacecraft, provides information on time and frequency of emission. The time and frequency at which the signal is received depend on the position and velocity of the spacecraft. In general two spacecraft will receive the same signal at different times and with different frequency shifts. If the CubeSats can measure, with reasonable accuracy, their relative position, the knowledge of the relative position between the two spacecraft in combination with the time and frequency difference of the received signal are sufficient to estimate the position and velocity with respect to the ground station. The paper explores two scenarios: one with two beacons and two receivers and one with a single beacon and more than two receivers. For the case in which a known minor body is in view of the camera, the paper will investigate the combination of TDOA measurements with the use of optical navigation.

The paper is organised as follows. First the dynamics and measurement models are introduced, followed by an analysis of the accuracy provided by different combinations of measurements. The reference case is a mission to the Moon. For a subset of measurements a second part of the paper analyses the use of an Unscented H-infinity Filter to estimate the state of the spacecraft.

DYNAMIC MODEL

The reference frame chosen for the simulation of the dynamical system and the navigation of the formation of spacecraft is a non-rotating reference frame, centred in the centre of mass of the Earth-Moon system (see Fig. 1). In such a frame, it is assumed that the motion of the principal

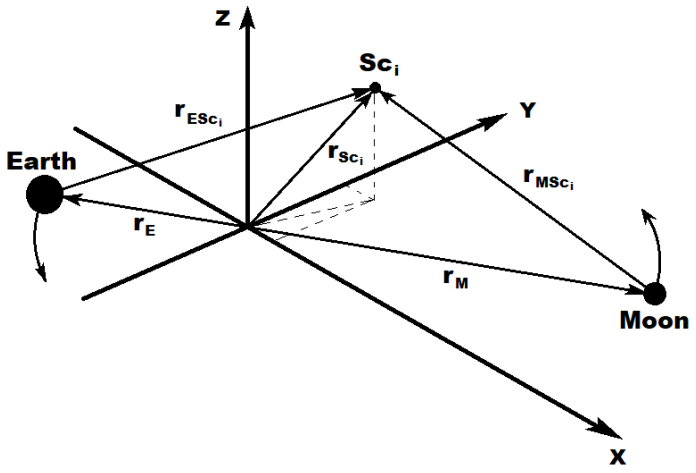

Figure 1. Reference frame for dynamics and measurement model.

bodies is known and consists of circular coplanar orbits with rotation period equal to the rotation period of the system. Both the Earth and Moon can rotate around their respective rotation axes. A further assumption is that both the primary bodies are considered to be homogeneous spheres.

With $\mathbf{r}_E$ as the position of the Earth, $\mathbf{r}_M$ as the position of the Moon and $\mathbf{r}_{Sc_i}$ the position of the i-th spacecraft all in the chosen reference frame, $\mathbf{r}_{ESc_i} = \mathbf{r}_{Sc_i} - \mathbf{r}_E$ and $\mathbf{r}_{MSc_i} = \mathbf{r}_{Sc_i} - \mathbf{r}_M$ as the relative position vectors from the i-th spacecraft to the Earth and the Moon respectively, the

nonlinear equations of motion are:

$$\ddot{\mathbf{r}}_{Sc_i} = -\frac{\mu_E}{\|\mathbf{r}_{ESc_i}\|^3}\mathbf{r}_{ESc_i} - \frac{\mu_M}{\|\mathbf{r}_{MSc_i}\|^3}\mathbf{r}_{MSc_i} \tag{1}$$

with μ_E and μ_M being the gravity constants of the Earth and the Moon respectively.

If one considers a formation of *n* spacecraft, the vector equation (1) can be applied to each spacecraft independently and can be re-written in compact form as a system of first order differential equations:

$$\dot{\mathbf{X}} = f(\mathbf{X}) \tag{2}$$

where $\mathbf{X} = [\mathbf{r}_{Sc_1}, \dot{\mathbf{r}}_{Sc_1}, \mathbf{r}_{Sc_2}, \dot{\mathbf{r}}_{Sc_2}, ..., \mathbf{r}_{Sc_n}, \dot{\mathbf{r}}_{Sc_n}]^T$ is the state vector containing the position and velocity of all the spacecraft.

MEASUREMENT MODEL

In this section we describe the type of measurements considered for the determination of position and velocity of the CubeSats with respect to one or more known beacons. Four types of measurements are considered: an optical measurement of a known object in space, the relative position and velocity via inter-satellite link, the Time Difference Of Arrival of the signal received from one or more beacons and the Doppler shift.

Optical Measurement Model

In order to develop the measurement model of the camera, two intermediate reference frames are required:

- Spacecraft coordinate system SC $\{x_{sc}\, y_{sc}\, z_{sc}\}$: the origin of this frame lies on the centre of mass of the spacecraft, with the three symmetrical body axes defined as three coordinate axes.[6]
- Camera coordinate system C $\{\hat{x}_C\, \hat{y}_C\, \hat{z}_C\}$: the centre C is the perspective projection of the camera, with the z_C-axis parallel to the optical axis of the camera and directed to the centre of the asteroid. The image plane is defined as O_C-$x_C\ y_C$.

In this paper, it is assumed that the body reference frame of each spacecraft is aligned with the camera and the attitude is known with a level of precision corresponding to that of the star tracker.

An image is generated according to the state of the system. Then, an ellipse fitting algorithm is used to compute the coordinates of the centroid of the asteroid in camera coordinates. Once the position of the centroid is known, the pointing angles can be computed by:

$$\varphi_C = \tan^{-1}\left(\frac{x_C}{f}\right);\ \psi_C = \tan^{-1}\left(\frac{y_C}{f/\cos(\varphi_C)}\right) \tag{3}$$

where f is the focal length of the camera. To these angles are added those required to go from the camera frame to the spacecraft frame. The model for the observation equations used in the filter, neglecting the contribution given by the attitude system, is:

$$\mathbf{z}_{camera} = \begin{bmatrix}\varphi \\ \psi\end{bmatrix} + \begin{bmatrix}\zeta_\varphi \\ \zeta_\psi\end{bmatrix} \tag{4}$$

where $\zeta_{\phi,\psi}$ comprise all the errors from attitude and the centroiding process. Note that here the illumination conditions are not considered, so it is assumed that each spacecraft sees the whole visible surface from its position. This is reasonable if one assumes that a complementary map could be built while starting the orbit acquisition, combining pictures from the whole formation.

Inter-spacecraft Measurements

The set of inter-spacecraft measurements is represented by the relative position vector between two spacecraft in the formation. This is composed of the relative distance, local azimuth and elevation.[7] The observation equation is given by:

$$\mathbf{z}_r = h_r\left(\mathbf{r}_{Sc_i},\ \mathbf{r}_{Sc_j}\right) = \left[d_r\ \varphi_r\ \psi_r\right]^T + \zeta_r \tag{5}$$

where $\zeta_r = \left[\zeta_{d_r}\ \zeta_{\varphi_r}\ \zeta_{\psi_r}\right]^T$ is the measurement noise. This simple measurement is providing the complete spacecraft-to-spacecraft vector in inertial space. Given spacecraft with state $\mathbf{x}_i$ and spacecraft with state $\mathbf{x}_j$ the spacecraft-to-spacecraft vector is $\mathbf{x}_{ij}$. In the case where the relative velocity is also computed, the measurement vector in equation (5) is extended by the relative velocity vector:

$$\mathbf{z}_{\dot{r}} = h_{\dot{r}}\left(\dot{\mathbf{r}}_{Sc_i},\ \dot{\mathbf{r}}_{Sc_j}\right) = \left[\dot{d}_r\ \dot{\varphi}_r\ \dot{\psi}_r\right]^T + \zeta_{\dot{r}} \tag{6}$$

where $\zeta_{\dot{r}} = \left[\zeta_{\dot{d}_r}\ \zeta_{\dot{\varphi}_r}\ \zeta_{\dot{\psi}_r}\right]^T$ is the measurement noise.

The error is due to the attitude error of the spacecraft and to the telemetry error. The pointing error is estimated to be about 1e-3 radians and the telemetry error is assumed to have comparable magnitude.

Time Of Arrival and Time Difference Of Arrival

For a source with coordinates $\mathbf{s}_j$ and a receiver with coordinates $\mathbf{r}_{Sc_1}$ the Time Of Arrival can be written as:

$$(t_1 - t_j) = \frac{1}{c}\sqrt{(\mathbf{r}_{Sc_1} - \mathbf{s}_j)^T(\mathbf{r}_{Sc_1} - \mathbf{s}_j)} \tag{7}$$

and if one squares both sides:

$$(t_1 - t_j)^2 = \frac{1}{c^2}(\mathbf{r}_{Sc_1}^T\mathbf{r}_{Sc_1} - \mathbf{s}_j^T\mathbf{x}_{Sc_1} - \mathbf{r}_{Sc_1}^T\mathbf{s}_j + \mathbf{s}_j^T\mathbf{s}_j) \tag{8}$$

If the same signal from s_j is received by a second spacecraft $\mathbf{r}_{Sc_2}$ we have:

$$(t_2 - t_j)^2 = \frac{1}{c^2}(\mathbf{r}_{Sc_2}^T\mathbf{r}_{Sc_2} - \mathbf{s}_j^T\mathbf{r}_{Sc_2} - \mathbf{r}_{Sc_2}^T\mathbf{s}_j + \mathbf{s}_j^T\mathbf{s}_j) \tag{9}$$

ans by subtracting (9) from (8) one gets the TDOA expression:

$$(t_2 - t_j)^2 - (t_1 - t_j)^2 = \frac{1}{c^2}(\mathbf{r}_{Sc_1}^T\mathbf{r}_{Sc_1} - \mathbf{r}_{Sc_2}^T\mathbf{r}_{Sc_2} - \mathbf{s}_j^T\mathbf{r}_{Sc_1} + \mathbf{s}_j^T\mathbf{r}_{Sc_2} - \mathbf{r}_{Sc_1}^T\mathbf{s}_j + \mathbf{r}_{Sc_2}^T\mathbf{s}_j) \tag{10}$$

where we have six unknowns. The inter-satellite link provides three equations that relate $\mathbf{r}_1$ to $\mathbf{r}_2$, therefore, the number of unknowns are reduced to three. Thus, with only two receivers and one beacon the problem cannot be completely solved and additional conditions are required. If two more stations are used as a beacon, then the problem becomes completely solvable.

Likewise if we had three receivers then the unknowns would be 9, the inter-satellite link would provide 6 equations and the TOA (or TDOA) other 3. In this case the problem can also be completely solved.

Frequency Of Arrival

If the receiver can measure the Doppler shift we can say that:

$$\Delta f_{i_1} \frac{c}{f_0} = \frac{(\mathbf{r}_{Sc_1} - \mathbf{s}_j)^T (\dot{\mathbf{r}}_{Sc_1} - \dot{\mathbf{s}}_j)}{r_1} \tag{11}$$

which introduces 3 additional unknowns. If one had two stations and two spacecraft then the Doppler equations would be 4 plus 3 equations giving the relative velocity via inter-satellite link. These 7 equations plus the 3 relative positions and 2 equations (10), one per station, allows one to completely solve the problem.

Note that even in this case if more than two stations or more than two spacecraft were available the Doppler shift would provide the velocities of the spacecraft with respect to the station provided that the inter-satellite link was giving the relative velocity among spacecraft.

Time and Frequency Error Estimations

The main problem with the use of the TOA is the drift of the internal clock of the receiver. In a two way communication system this error can be eliminated by synchronisation of the on board and ground clocks. However, in a one way communication solution the spacecraft needs to reset its clock only using the reference signal coming from ground.

We assume that the formation is able to synchronise their clocks using a standard two way communication system and standard clock synchronisation algorithm, such as Barkley's algorithm or equivalent. This synchronisation however, does not avoid a possible drift of all the clocks. If the clocks are well characterised, one can assume that the model can be used to filter the drift and correct the TOA. Although this is a reasonable assumption here we provide also a reset mechanism to partially synchronise the clocks on board with the source.

The idea is based on a heart-beat concept in which the receiver compares the local time increments with the reference time increment transmitted by the ground station. If one calls t_0 the exact universal time of the ground station and t_l the local time on the spacecraft, the spacecraft is expected to receive a first pulse at time t_{l1} corresponding to a transmission time t_{01}. After a time interval Δt_0 the ground station sends a second pulse. When the pulse is received the spacecraft register the time t_{l2} such that:

$$t_{l2} = t_{l1} + \Delta t_0 + \frac{\Delta r}{c} + \epsilon_{_{TOA}} \tag{12}$$

where $\Delta t_l = t_{l2} - t_{l1}$ is the Time Difference Of Arrival at the same spacecraft, Δr is the displacement in the direction of propagation of the radio wave, and $\epsilon_{_{TOA}}$ is the accumulated error of the clock on board.

If the frequency at which the two clocks are synchronised is high, Δt_0 is small and one can assume a linear model for the displacement such that:

$$\Delta t_l = \Delta t_0 + \frac{\dot{r}\Delta t_0}{c} + \epsilon_{_{TOA}} \tag{13}$$

The local velocity can be derived from the Frequency Of Arrival:

$$\dot{r} = \frac{\Delta f c}{f_0} + \epsilon_{_{FOA}} \tag{14}$$

From which one has that:

$$\epsilon_{TOA} = \Delta t_l - \Delta t_0 - \frac{\Delta f \Delta t_0}{f_0} - \frac{\epsilon_{FOA} \Delta t_0}{c} \tag{15}$$

The error in velocity ϵ_{FOA} depends on the error in the Doppler shift measurement. This error depends on the observation time T_o, and can be approximated to be $1/T_o$. In order to remove the drift accumulated in the time interval Δt_0 the ratio ϵ_{FOA}/c has to be smaller than the expected drift of the clock. For a standard clock the expected drift is 1e-6 per second, which gives a required accuracy of the Doppler measurement of less than 300 m/s or 12kHz assuming a carrier in X band at 12GHz. This accuracy only requires an observation time of 8.3276e-5s. Having said that, it is desirable to reduce the error in TOA down to less than a millisecond, as will be shown later. In this case we can impose a Doppler error of 1 m/s that corresponds to 40Hz and an observation time of 2.42e-2s.

Note that additional corrections are required to account for the acceleration acting on the spacecraft that has an impact on Δr. For example at the Earth-Moon distance the acceleration on the spacecraft introduces a difference in Δr of about 1.3e-4 m over 10s and a prediction error of 4.5e-13s.

MEASUREMENT ANALYSIS

In this section we analyse the precision provided by different combinations of measurements. In particular we consider the following cases:

1. Three spacecraft and one station. The station provides three TOA that are combined with two inter-satellite links.

2. This case is as before but also considers the case in which the spacecraft use the TDOA instead of the TOA in combination with one optical observation.

3. Two spacecraft and two stations. The stations provide two TOA and four Doppler shifts that are combined with one inter-satellite link.

In all the following tests the spacecraft are at a relative distance of 200km and are maintained on a plane perpendicular to the x-axis. The TOA and FOA equations are solved with a Newton iteration with analytical Jacobian matrix and Levenberg-Marquardt step-length control. In order to mitigate the effect of numerical inaccuracies, the equations are scaled by pre-multiplication using the estimated distance between spacecraft 1 and station 1. This scaling allows for accurate convergence even with short spacecraft-to-spacecraft bases down to a few tens of km at the Earth-Moon distance.

All results correspond to the average over 100 simulations. For each simulation, the measurement error is generated by multiplying the 1 σ value times a random number drawn from a normal distribution with zero mean and variance equal to 1. The TOA drift is a constant bias equal to 1e-6s per second on top of which we apply a 1 σ error noise of 1e-7s. The minimum 1 σ noise for the spacecraft-to-spacecraft pointing accuracy is 1e-3 radians and the maximum is 0.1 radians, while we consider a maximum Doppler shift noise of 40Hz and a 1 σ optical measurement noise of 3e-3 radians.

Case 1: 3 spacecraft 1 station

In the case of 3 spacecraft flying in formation and one station, the signal produced by the station is received at three different TOAs by the three spacecraft. The three spacecraft maintain a knowledge of their relative position and local time by inter-satellite link and synchronization of the clocks. In this analysis spacecraft number 1 maintains its clock synchronized with the ground station using the technique presented in the previous section. The first analysis places the spacecraft at the Earth-Moon distance and evaluates the sensitivity of the estimated position of spacecraft 1, with respect to the Earth, to the error in the measurement of the the TOA and of the inter-satellite position vector. The result can be seen in Figure 2. The figure shows that the correction on the TOA is effective and the main source of error is the inter-satellite position. In this case the error in pointing accuracy is pushed to 0.1 radians. It should be noted that the error depends on the geometry with which the station is seen by the three spacecraft.

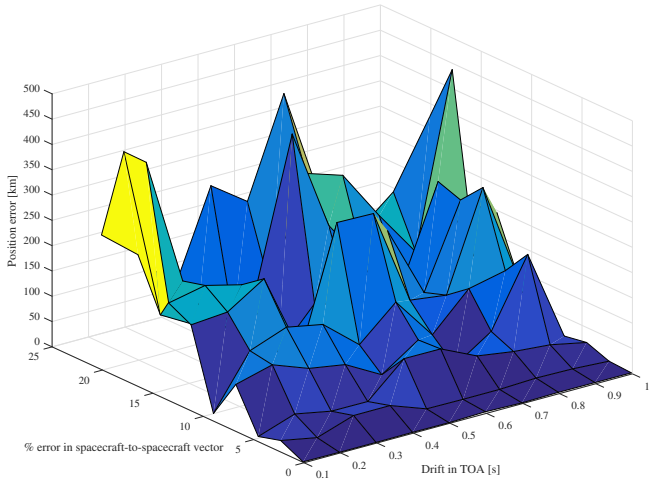

Figure 2. Estimated position error vs TOA and pointing errors

In order to partially test the sensitivity to the change in geometry we simulated a transfer from a LEO (300 km altitude) to the Moon. The measurements start at the GEO distance. Figs. 3 and 4 show the estimation error along the trajectory for the min and max pointing accuracy, where the minimum pointing error is 1e-3 radians. Fig. 5 shows the estimated vs the true trajectory for the case of the maximum error in pointing accuracy.

Case 2: 3 spacecraft 1 station and one optical measurement

The case of three spacecraft can be revisited considering the TDOA instead of the TOA. In this case the correction on the TOA is not necessary as it is compensated for by the synchronization of the local clocks. On the other hand a solution of the system of three TDOA and six inter-satellite link equations yields a result that is not unique in three dimensions. A fourth spacecraft or a second station would be required. In this test, instead, we consider an additional optical measurement.

In the case of a close approach to a known body a limb fitting measurement would provide the required additional information, however that would not provide a good measurement when in deep

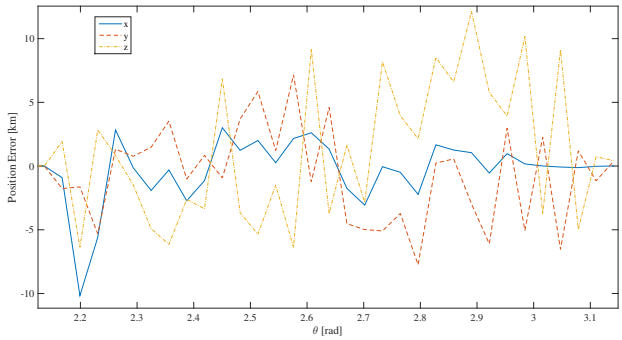

Figure 3. Case 1: Position error along the Earth-Moon transfer considering a pointing accuracy of 1e-3 radians

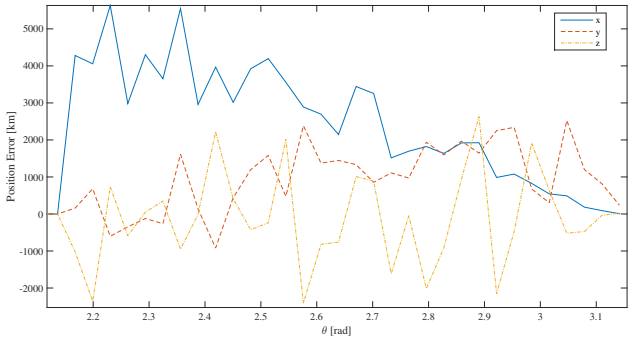

Figure 4. Case 1: Position error along the Earth-Moon transfer considering a pointing accuracy of 1e-1 radians

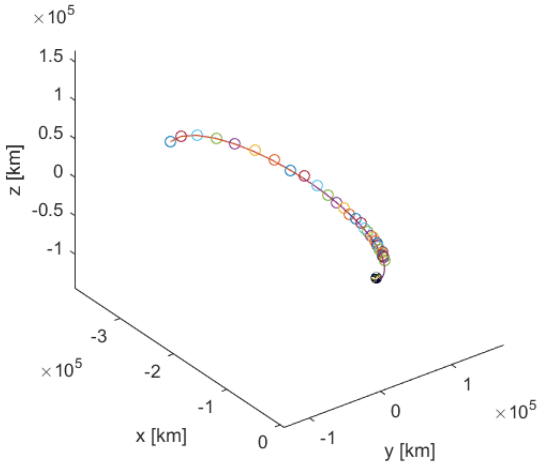

Figure 5. Case 1: Estimated trajectory (circles) vs true trajectory (solid line) considering a pointing accuracy of 1e-1 radians

space. The additional measurement comes only from the pointing of the camera towards a known body with known ephemerides. In this case the Moon. The error in the pointing of the camera is the combination of the attitude pointing accuracy and the pixelation error (additional effects like aberration of the optics are not considered) and was set to 3e-3 radians in the following example.

Fig. 7 shows the estimation error when the inter-satellite pointing error is 1e-3 radians while Fig. 6 shows the estimated trajectory vs the true one when the pointing error is pushed to 0.1 radians. In both cases the optical measurement is 3e-3 radians. The two spikes in Fig. 7 are two outliers and can be filtered out if the estimation considers an extended arc of measurements.

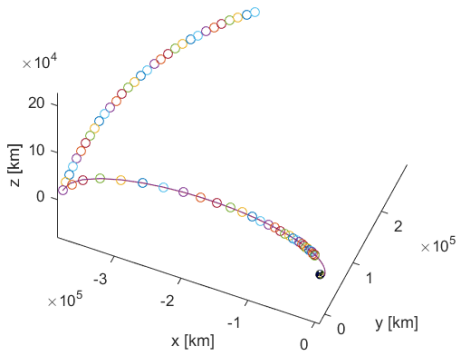

Figure 6. Case 2: Estimated trajectory including optical measurements and TDOA for a pointing accuracy of 1e-1 radians

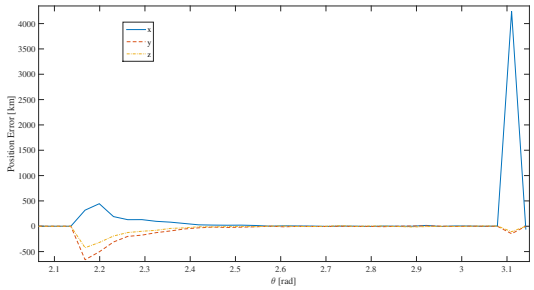

Figure 7. Case 2: Position error along the Earth-Moon transfer considering a pointing accuracy of 1e-3 radians and a combination of TDOA and optical measurements

Case 3: 2 spacecraft 2 stations

In the case of only two spacecraft, the time of arrival is not sufficient to determine the complete position vector. In two dimensions if the TOA is combined to calculate the TDOA the locus of all possible positions of the station with respect to the two spacecraft is a hyperbola. In order to get the complete state vector of the two spacecraft we first assume that the relative velocity vector between two spacecraft can be measured with the same accuracy as the relative position vector. Then a complete solution can be computed by adding a second emitting station, synchronized with the first, and the FOA.

Figure 8 shows the sensitivity to the pointing accuracy and TOA measurement for the worst FOA. Given that the FOA can be measured quite accurately, even in this case the major problem comes from the pointing accuracy. Figures 9 and 10 show the estimated position and velocity errors of

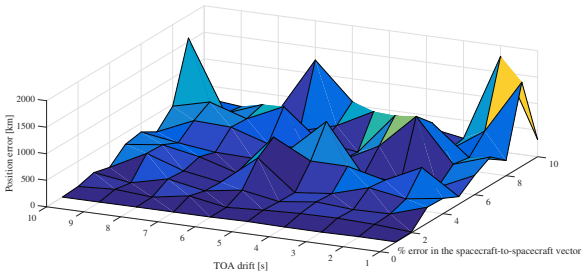

Figure 8. Case 3: Estimated position error vs errors in TOA and pointing accuracy for the maximum error is Doppler measurement of 40Hz

spacecraft 1 for the case of maximum pointing error. The figures demonstrate that the error in pointing accuracy is critical in this case and needs to be limited to less than 0.1 radians to get a reasonable estimation of the position but more importantly of the velocity. The resulting estimated trajectory can be found in Fig. 11.

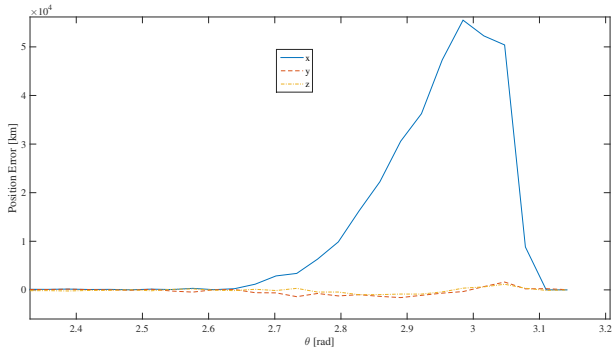

Figure 9. Case 3: Position error along the Earth-Moon transfer considering a pointing accuracy of 1e-1 radians

Figures 12 and 13 show the estimated position and velocity errors of spacecraft 1 for the case of minimum pointing error of 1e-3 radians. In this case the result is acceptable both in position and velocity along the whole transfer.

STATE ESTIMATION AND FILTERING

The measurement analysis in previous sections does not consider any filtering of the error or the acquisition of multiple measurements over extended arcs. In this section we introduce some of the measurement combinations into a sequential filtering process.

The state estimation process is based on the same Unscented H_∞ Filter proposed in.[7] The UHF works on the premise that one can find a good approximation for the *a posteriori* covariance by propagating a limited set of optimally chosen samples.[8] Using the estimation theory formalism, the nonlinear process in Eq. (2) and the measurement equations can be discretised in time and written

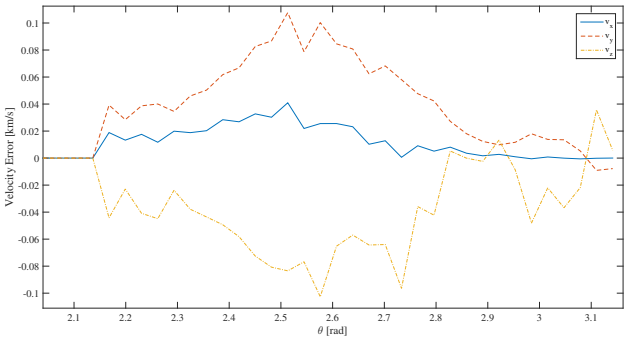

Figure 10. Velocity error along the Earth-Moon transfer considering a pointing accuracy of 1e-1 radians

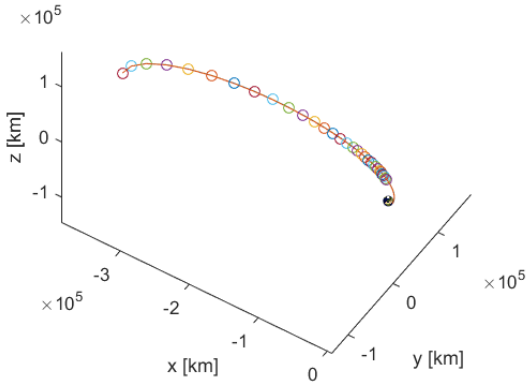

Figure 11. Case 3: Estimated trajectory (circles) vs true one (solid line) considering a pointing accuracy of 1e-1 radians

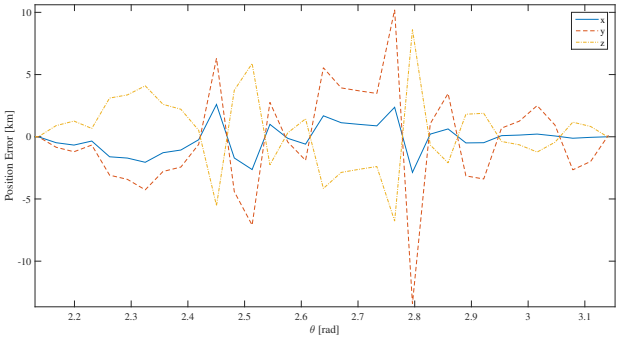

Figure 12. Case 3: Position error along the Earth-Moon transfer considering a pointing accuracy of 1e-3 radians

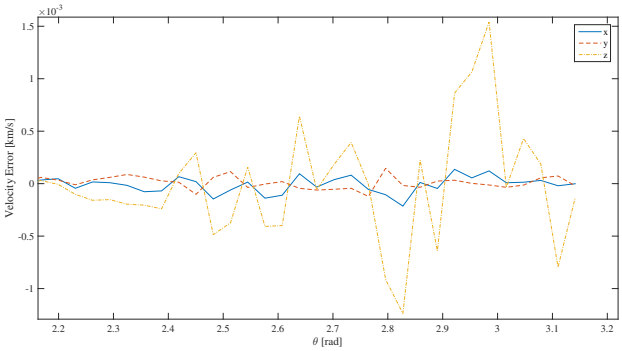

Figure 13. Case 3: Velocity error along the Earth-Moon transfer considering a pointing accuracy of 1e-3 radians

as:

$$\begin{aligned} \mathbf{x}_{k+1} &= f\left(\mathbf{x}_k\right) \\ \mathbf{y}_k &= h\left(\mathbf{x}_k\right) \end{aligned} \tag{16}$$

where $\mathbf{v}_k$ is the measurement noise. The initial conditions are the estimated position and velocity from the filter at time t_k. The UHF relies on the unscented transformation to propagate a set of suitable sigma points, drawn from the *a priori* covariance matrix. The set of sigma points χ are given as:

$$\chi_i = \begin{cases} \tilde{\mathbf{x}}_k & i = 0 \\ \tilde{\mathbf{x}}_k + \left(\sqrt{\left(n + k_{UHF}\right)\mathbf{P}_k + \mathbf{Q}}\right)_i & i = 1,\ 2,\ ...,\ n \\ \tilde{\mathbf{x}}_k - \left(\sqrt{\left(n + k_{UHF}\right)\mathbf{P}_k + \mathbf{Q}}\right)_i & i = n+1,\ ...,\ 2n \end{cases} \tag{17}$$

where χ is a matrix consisting of (2n+1) vectors with $k_{UHF} = \alpha_{UHF}^2\left(n + \lambda_{UHF}\right) - n$, where k_{UHF} is a scaling parameter, and constant α_{UHF} determines the extension of these vectors around $\tilde{\mathbf{x}}_k$. We set α_{UHF} equal to 10^{-2} and λ_{UHF} is set equal to (3n). The sigma points are transformed or propagated through the nonlinear function, the so-called unscented transformation. The predicted mean of the state vector $\tilde{\mathbf{x}}_k^-$, the covariance matrix $\tilde{\mathbf{P}}_k^-$, and the mean observation $\tilde{\mathbf{y}}_k^-$ can be approximated using the weighted mean and covariance of the transformed vectors:

$$
\begin{aligned}
&\chi^{i}_{k|k-1} = f\left(\chi^{i}_{k-1},\ \mathbf{u}_k\right)\\
&\tilde{\mathbf{x}}^{-}_{k} = \sum_{i=0}^{2n} W^{(m)}_{i}\chi^{i}_{k|k-1}\\
&\mathbf{P}^{-}_{k} = \sum_{i=0}^{2n} W^{(c)}_{i}\left[\chi^{\mathbf{i}}_{\mathbf{k|k-1}} - \tilde{\mathbf{x}}^{-}_{k}\right]\left[\chi^{\mathbf{i}}_{\mathbf{k|k-1}} - \tilde{\mathbf{x}}^{-}_{k}\right]^{T} + \mathbf{Q}\\
&\mathbf{Y}^{i}_{k|k-1} = h\left(\chi^{i}_{k|k-1}\right)\\
&\tilde{\mathbf{y}}^{-}_{k} = \sum_{i=0}^{2n} W^{(m)}_{i}\mathbf{Y}^{i}_{k|k-1}
\end{aligned}
\tag{18}
$$

where $W^{(m)}_{i}$ and $W^{(c)}_{i}$ are the weighted sample mean and covariance given by:

$$
\begin{aligned}
W^{(m)}_{0} &= k_{_{UHF}}/(n + k_{_{UHF}})\\
W^{(c)}_{0} &= k_{_{UHF}}/(n + k_{_{UHF}}) + (1 - \alpha^{2}_{_{UHF}} + \beta_{_{UHF}})\\
W^{(m)}_{i} &= W^{(c)}_{i} = k_{_{UHF}}/[2(n + k_{_{UHF}})], \quad i = 1,\ 2,\ ...,\ 2n
\end{aligned}
\tag{19}
$$

and $\beta_{_{UHF}}$ is used to incorporate prior knowledge of the distribution with $\beta_{_{UHF}} = 2$.[9] The updated covariance $\mathbf{P}_{y,k}$ and the cross correlation matrix $\mathbf{P}_{xy,k}$ are:

$$
\begin{aligned}
\mathbf{P}_{y,k} &= \sum_{i=0}^{2n} W^{(c)}_{i}\left[\mathbf{Y}^{\mathbf{i}}_{\mathbf{k|k-1}} - \tilde{\mathbf{y}}^{-}_{k}\right]\left[\mathbf{Y}^{\mathbf{i}}_{\mathbf{k|k-1}} - \tilde{\mathbf{y}}^{-}_{k}\right]^{T} + \mathbf{R}\\
\mathbf{P}_{xy,k} &= \sum_{i=0}^{2n} W^{(c)}_{i}\left[\chi^{\mathbf{i}}_{\mathbf{k|k-1}} - \tilde{\mathbf{x}}^{-}_{k}\right]\left[\mathbf{Y}^{\mathbf{i}}_{\mathbf{k|k-1}} - \tilde{\mathbf{y}}^{-}_{k}\right]^{T}
\end{aligned}
\tag{20}
$$

Finally, the filter state vector $\tilde{\mathbf{x}}_k$ and covariance updated matrix $\mathbf{P}_{x,k}$ are represented as follows:

$$
\begin{aligned}
&\tilde{\mathbf{x}}_k = \tilde{\mathbf{x}}^{-}_{k} + \mathbf{K}\left(\mathbf{y}_k - \tilde{\mathbf{y}}_k\right)\\
&\left(\mathbf{P}^{+}_{k}\right)^{-1} = \left(\mathbf{P}^{-}_{k}\right)^{-1} + \left(\mathbf{P}^{-}_{k}\right)^{-1}\mathbf{P}_{xy,k}\mathbf{R}^{-1}\left[\left(\mathbf{P}^{-}_{k}\right)^{-1}\mathbf{P}_{xy,k}\right]^{T} - \vartheta_k\mathbf{I}_d\\
&\mathbf{K} = \mathbf{P}_{xy,k}\mathbf{P}^{-1}_{y,k}
\end{aligned}
\tag{21}
$$

where $\mathbf{K}$ is the Kalman gain matrix, ϑ_k is the performance bound of the H_∞ filter, and R_k is a suitable matrix which, in the case of a normal distribution, coincides with the measurement noise covariance matrix at time step k. In order to assure that the covariance matrix is positive definite this value is calculated at each iteration as:

$$
\vartheta^{-1}_{k} = \xi max\left(eig\left(\left(\mathbf{P}^{-}_{k}\right)^{-1} + \left(\mathbf{P}^{-}_{k}\right)^{-1}\mathbf{P}_{xy,k}\mathbf{R}^{-1}\left[\left(\mathbf{P}^{-}_{k}\right)^{-1}\mathbf{P}_{xy,k}\right]^{T}\right)^{-1}\right)
\tag{22}
$$

As one can see from the set of equations (21), the performance bound has no direct effect on the calculation of the gain and on the update step for the estimated state. Nonetheless ϑ_k modifies the shape of covariance matrix update, which, in turn, generates a different distribution of the sigma

points. In this way, the propagation and the update step at the following time step will be directly influenced by the value of the performance bound.

CASE STUDIES

The test case scenario chosen to show the results is set as follows. Both the Earth and the Moon start with their position lying on the x-axis of the principal reference frame. The initial attitude of the Earth is such that the principal meridian (Greenwich) intersects the x-axis of the Earth-Moon direction and its rotation axis is tilted in the same direction. Two ground stations are considered and their locations and characteristics are listed in Table 1, with T_0 being the period of transmission of the signal and f_0 the frequency of the carrier.

Table 1. Ground stations parameters

	Lat [deg]	Lon [deg]	Alt [m]	T_0 [s]	f_0 [GHz]
Malargüe	35.776 S	69.398 W	1550	120	12.0
Gatineau	45.585 N	75.807 W	2126	120	12.0

Table 2. Orbital elements for spacecraft 1

a [km]	e	i [deg]	Ω [deg]	ω [deg]	ν_0 [deg]
8634.751	0	90	180	N/D	-90

The members of the formation of spacecraft are placed in circular polar orbits around the Moon. The initial conditions are defined with Keplerian orbital elements for spacecraft 1 and relative Cartesian coordinates for the other members of the formation. Table 2 reports the orbital elements of spacecraft 1 with respect to the Moon, with the initial true anomaly, ν_0, being referred to the position of the ascending node. The value for the semi-major axis is chosen to ensure an orbital period of 20 hours. The initial conditions for the other members of the formation will be given in the respective case section.

All the spacecraft independently estimates the states of the whole formation. The first guess initial conditions for each spacecraft are set to be equal to the real initial states with the addition of a bias in both position and velocity; the initial covariance matrices are diagonal matrices with elements equal to the square root of two times the values of the aforementioned biases (Table 3).

Table 3. Biases on the initial estimate state and initial covariance matrix for each spacecraft

	$x\ [km]$	$y\ [km]$	$z\ [km]$	$\dot{x}\ [m/s]$	$\dot{y}\ [m/s]$	$\dot{z}\ [m/s]$
$X_0^{est} - X_0$	10	10	10	1	1	1
	$x\ [km^2]$	$y\ [km^2]$	$z\ [km^2]$	$\dot{x}\ [km^2/s^2]$	$\dot{y}\ [km^2/s^2]$	$\dot{z}\ [km^2/s^2]$
$diag(P_0)$	$4e2$	$4e2$	$4e2$	$4e-6$	$4e-6$	$4e-6$

The following case studies and combinations of measurements will be considered. Note that the initial estimation error is comparable to the one achieved in the measurement analysis when the pointing accuracy is about 1e-3 radians. In addition it is assumed that the clocks are synchronised as explained in the dedicated section.

1. Three spacecraft and one station. The station provides three TOA that are combined with two inter-satellite links.

2. Two spacecraft and two stations. The stations provide four TOA and four Doppler shifts that are combined with one inter-satellite link.

For each scenario, results are shown for inter-spacecraft distance of about 100km and 200km.

Case 1.1: 1 ground station, 3 spacecraft, TOA, 100km

In this test case, the ground station used is the one located at Malargüe. The initial relative states of the members of the formation with respect to spacecraft 1 are listed in Table 4.

Table 4. Relative states of the members of the formation with respect to spacecraft 1

	$\Delta x\ [km]$	$\Delta y\ [km]$	$\Delta z\ [km]$	$\Delta \dot{x}\ [m/s]$	$\Delta \dot{y}\ [m/s]$	$\Delta \dot{z}\ [m/s]$
Spacecraft 2	0	0	-100	0	0	0
Spacecraft 3	0	-100	-100	0	0	0

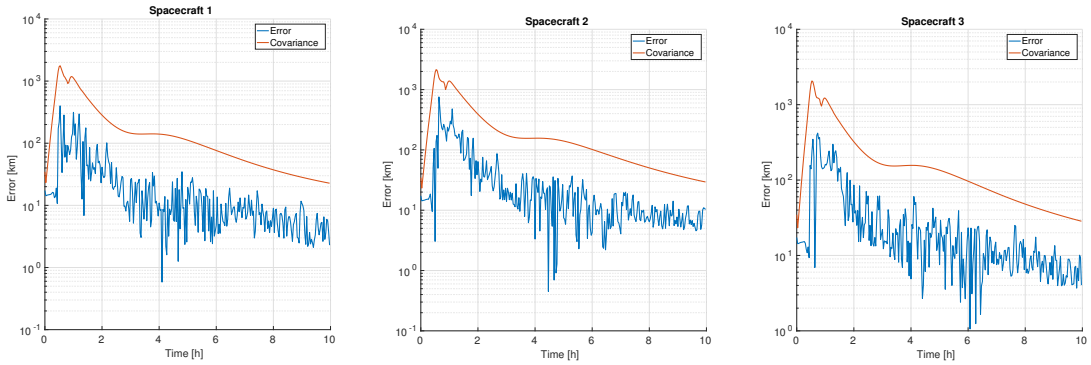

Figure 14. Case 1.1: position errors for the formation

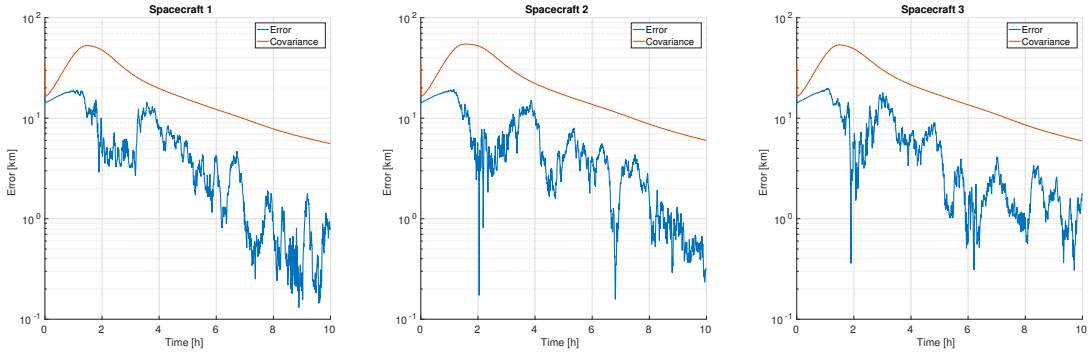

Figure 15. Case 1.1: position errors for the formation with measurements every 30 seconds

Figure 14 shows the evolution of the estimate on the position error and the expected covariance at 1-σ for all the spacecraft. It can be seen that all the spacecraft show similar trends. During the first hour the estimation error increases of an order of magnitude before starting decreasing again and reaching the same value of the beginning at around the third hour. Then it constantly decreases

reaching values below 10km. Figure 15 shows the results for the same test case when the ground station transmits the beacon every 30 seconds. In this case, the initial increment in the estimation is much lower than in the previous case and also the final values are of the order of 1km, with spacecraft 2 reaching error levels in the hundreds of meters.

Case 1.2: 1 ground station, 3 spacecraft, TOA, 200km

The initial relative states of the members of the formation with respect to spacecraft 1 are listed in Table 5, while Figures 16 and 17 show the position errors for transmission intervals of 2 minutes and 30 seconds respectively.

Table 5. Relative states of the members of the formation with respect to spacecraft 1

	$\Delta x\ [km]$	$\Delta y\ [km]$	$\Delta z\ [km]$	$\Delta \dot{x}\ [m/s]$	$\Delta \dot{y}\ [m/s]$	$\Delta \dot{z}\ [m/s]$
Spacecraft 2	0	0	-200	0	0	0
Spacecraft 3	0	-170	-100	0	0	0

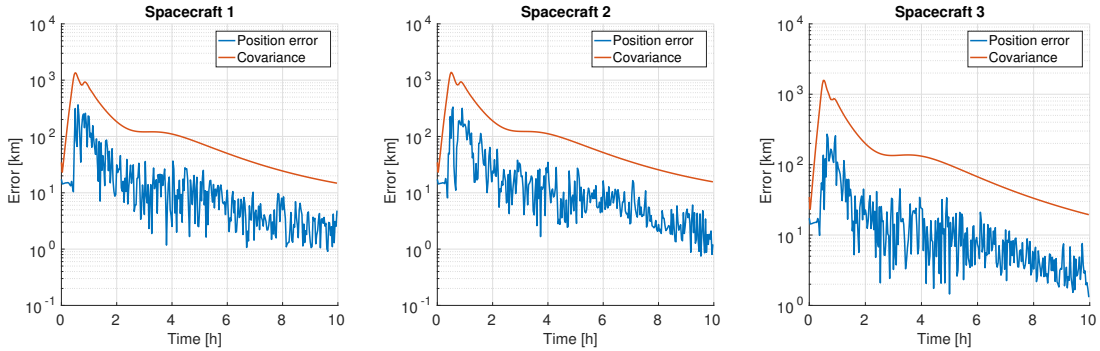

Figure 16. Case 1.2: position errors for the formation

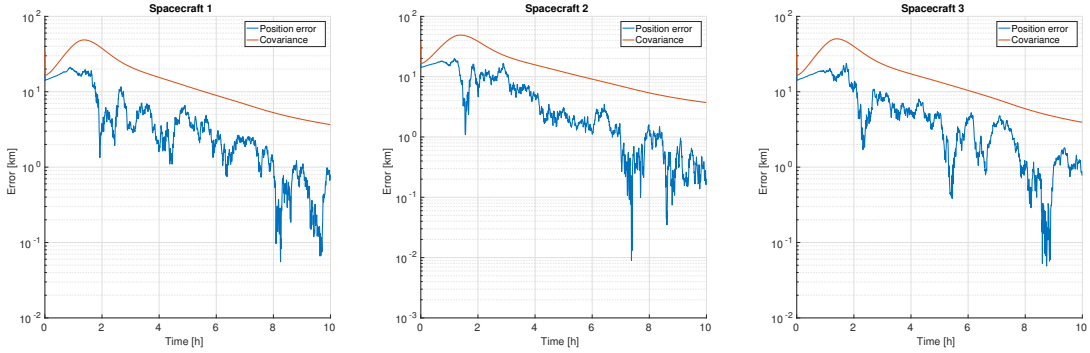

Figure 17. Case 1.2: position errors for the formation with measurements every 30 seconds

When comparing with the previous case (Figures 14 and 15) there is perfect agreement in the trend of the estimation errors. However, the final values obtained in this case with transmission period of 2 minutes are smaller than with an inter-satellite separation of 100km.

Case 2.1: 2 ground stations, 2 spacecraft, TOA and FOA, 100km

In this test case, both the ground stations are used and the initial relative state of spacecraft 2 with respect to spacecraft 1 is listed in Table 6.

Table 6. Relative state of spacecraft 2 with respect to spacecraft 1

	$\Delta x\ [km]$	$\Delta y\ [km]$	$\Delta z\ [km]$	$\Delta \dot{x}\ [m/s]$	$\Delta \dot{y}\ [m/s]$	$\Delta \dot{z}\ [m/s]$
Spacecraft 2	0	0	-100	0	0	0

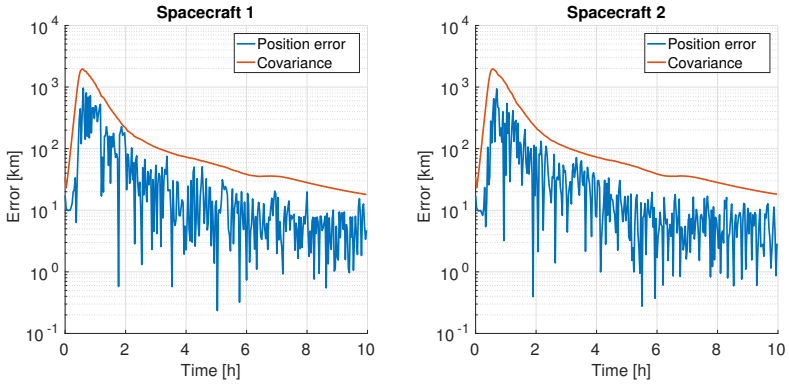

Figure 18. Case 2.1: position errors for the formation

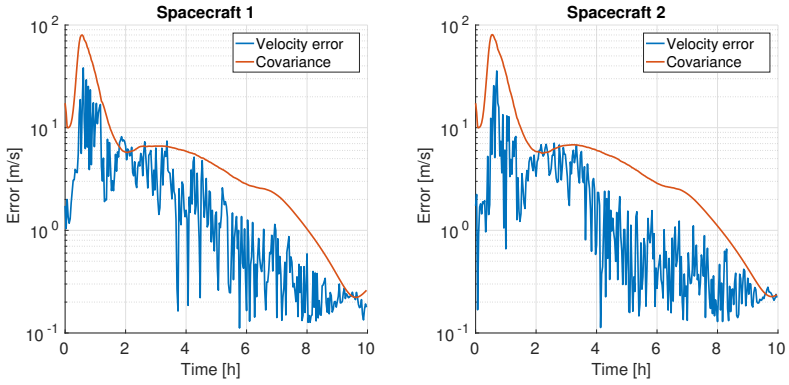

Figure 19. Case 2.1: velocity errors for the formation

Figures 18 and 19 show the position and velocity estimation errors for this test case. Comparing the results in position with the ones shown in Figure 14, it can be noted that, in both the scenarios, the position estimation errors follow the same trends. This indicates that the performances obtained using 3 spacecraft and 1 station can be obtained exchanging one spacecraft with a ground station. The estimate on the velocity errors gives good performances, with final values around 0.2m/s. Even in this scenario, reducing the time interval in the transmission of the signals from the stations to 30 seconds improves the performances of the estimation process. The results shown in Figure 20 have the same behaviour as those of Figure 15, with final values of the estimation error mainly between 100m and 1km. The estimate on the velocity errors are reduced by one order of magnitude.

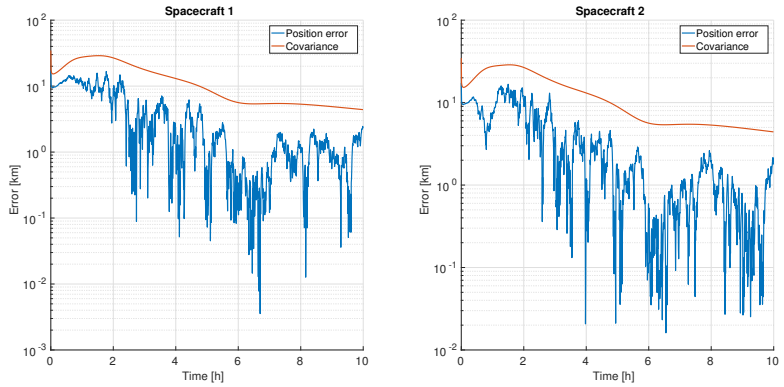

Figure 20. Case 2.1: position errors for the formation with measurements every 30 seconds

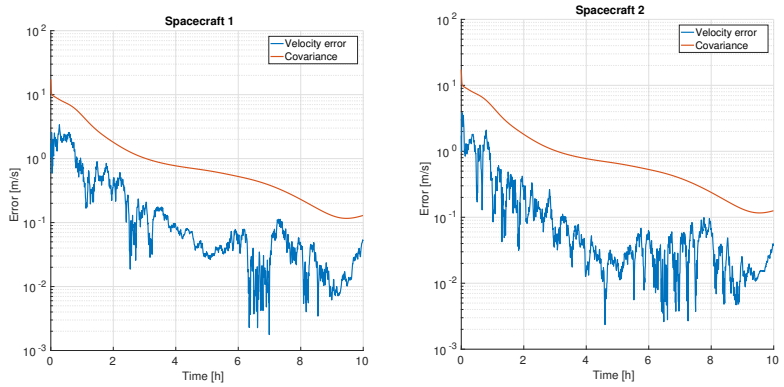

Figure 21. Case 2.1: velocity errors for the formation with measurements every 30 seconds

Case 2.2: 2 ground stations, 2 spacecraft, TOA and FOA, 200km

The initial relative state of spacecraft 2 with respect to spacecraft 1 is listed in Table 7.

Table 7. Relative state of spacecraft 2 with respect to spacecraft 1

	$\Delta x\ [km]$	$\Delta y\ [km]$	$\Delta z\ [km]$	$\Delta \dot{x}\ [m/s]$	$\Delta \dot{y}\ [m/s]$	$\Delta \dot{z}\ [m/s]$
Spacecraft 2	0	0	-200	0	0	0

Comparing Figures 22 and 23 with Figures 18 and 19 shows that the difference in separation between the spacecraft produce similar results. Comparing Figures 24 and 25 with Figures 20 and 21 confirms that higher frequency in the transmission of the signals from the stations can improve the performances of the estimation process.

FINAL REMARKS

The paper presented an analysis of the accuracy in position and velocity estimation for a small formation of CubeSats beyond LEO. The underlying assumption is that only one way communications from groundstation to CubeSat are available and the formation has to estimate their position

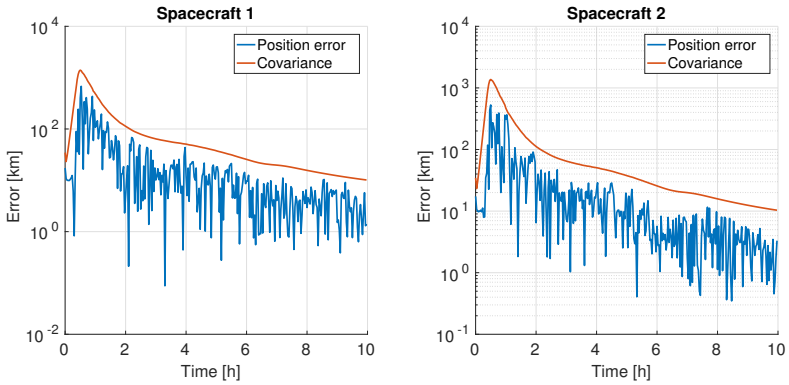

Figure 22. Case 2.2: position errors for the formation

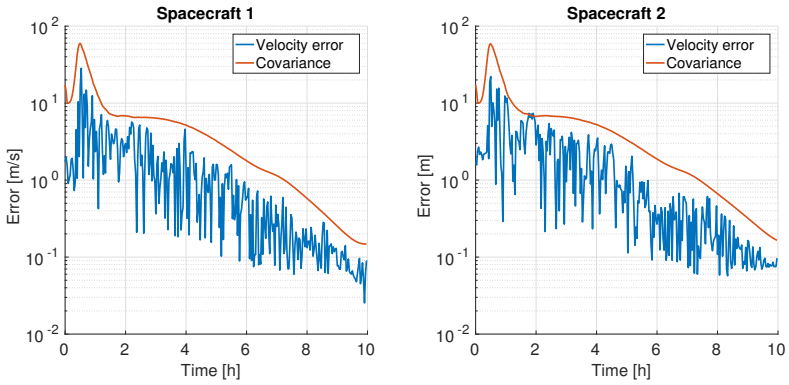

Figure 23. Case 2.2: velocity errors for the formation

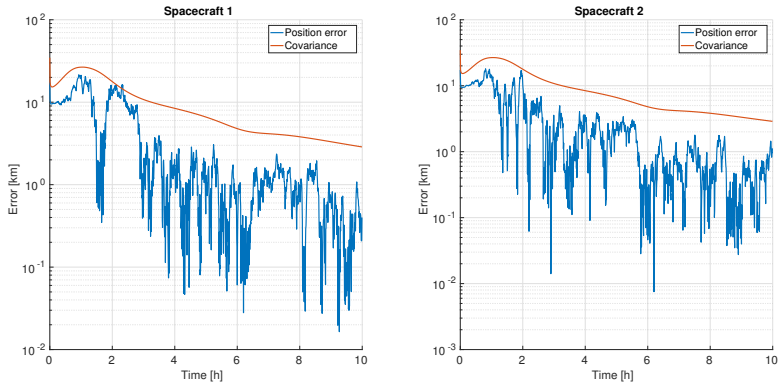

Figure 24. Case 2.2: position errors for the formation with measurements every 30 seconds

and velocity autonomously. The paper explored different combinations of measurements taking into account that a CubeSat has limited resources and low cost components, including on-board clock and camera. It was found that if the CubeSats are placed at a relative distance of 200 to 300 km and the pointing accuracy is 1e-3 radians, the inertial position vector can be well estimated in deep space using a single station as beacon. A good level of accuracy can also be obtained by combin-

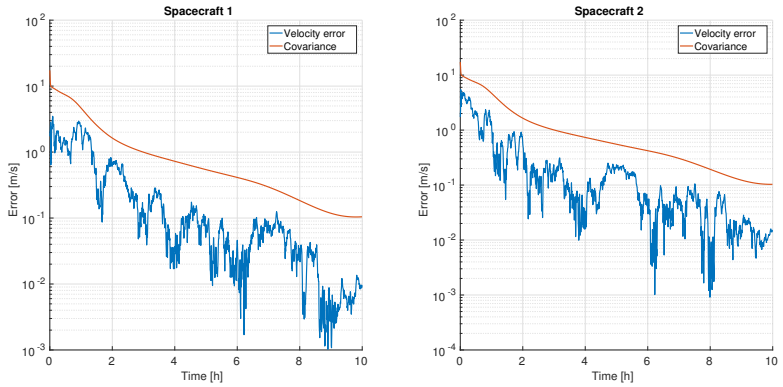

Figure 25. Case 2.2: velocity errors for the formation with measurements every 30 seconds

ing TDOA measurements and optical observations of the Moon although this approach seems to be more expensive and more sensitive to geometry of the formation with respect to the beacons. With two stations and the inclusion of Doppler measurements the velocity can be estimated down to a few meters per second. A coarser pointing accuracy of up to 0.1 radians, instead, leads to very poor results in this case. These results were obtained with no filtering or minimisation of the estimation error over extended arcs. On the contrary they correspond to point-wise measurements without accounting for the dynamics of the spacecraft and the initial orbit determination. The inclusion of multiple measurements can further improve the estimation of position and velocity.

The inclusion of TOA and FOA in a UHF provided further improvement in the estimation of the state of the formation with errors that reduces below 1km in position.

Future work will be dedicated to further extend this techniques to longer distances from the source. In this case the convergence of the solution for small relative position vectors becomes rather difficult.

REFERENCES

[1] M. Sami Asmar, Steve, "Mars Cube One (MarCO) - The First Planetary CubeSat Mission ," *Jet Propulsion Laboratory NASA Report 2014*, 2015.

[2] D. J. Torrieri, "Statistical Theory of Passive Location Systems," *IEEE Transactions on Aerospace and Electronic Systems*, Vol. 20, No. 2, March 1984.

[3] R. Ulman, "Motion detection using TDOA and FDOA measurements," *IEEE Transactions on Aerospace and Electronic Systems*, Vol. 37, No. 2, April 2001.

[4] K. Ho and Y. Chan, "Geolocation of a Known Altitude Object From TDOA and FDOA Measurements," *IEEE Transactions on Aerospace and Electronic Systems*, Vol. 33, No. 3, July 1997.

[5] J. Mason, "Algebraic two-satellite TOA/FOA position solution on an ellipsoidal Earth," *IEEE Transactions on Aerospace and Electronic Systems*, Vol. 40, No. 3, July 2004.

[6] S. Li, P. Y. Cui, and H. T. Cui, "Vision-aided inertial navigation for pinpoint planetary landing," *Aerospace Science and Technology*, Vol. 11, No. 6, 2007.

[7] M. Vetrisano and M. Vasile, "Autonomous Navigation of a Spacecraft Formation in the Proximity of an Asteroid," *Advances in Space Research*, Vol. 57, No. 8, 2016.

[8] S. J. Julier, J. K. Uhlmann, and H. F. Durrant-Whyte, "A new approach for filtering nonlinear systems," *In proceedings of the American Control conference, Seattle, Washington*, 1995.

[9] J. L. Crassidis and J. L. Junkins, *Optimal Estimation of Dynamic Systems*. Chapman and Hall/CRC Press, Boca Raton, FL, 1st edition ed., 2004.